Calculations of the Energy and Mass Yields from the Thermal-Neutron Fission of U^{235}

J. M. Ferguson and P. A. Read
U. S. Naval Radiological Defense Laboratory, San Francisco, California
(Received 1 April 1966)

Improvements in a semiempirical correlation of the energy and mass yield data for U^{236} fission are presented. The available mass, energy, and neutron-emission data are correlated with each other within the accuracy of the input data. A simple model of the U^{236} fragments at scission is presented. This model, together with some experimental data, is used to predict the surface-tension parameters of the fragments and kinetic energies of the fragment pairs. The calculated kinetic energies agree reasonably well with experiment. The surface-tension parameters of the fragments show strong shell effects, as indicated in other studies. The shapes of the fragments at scission are estimated from the model.

I. INTRODUCTION

In this paper two somewhat separate calculations are presented. In Sec. II we bring up to date an empirical correlation of U^{236} fragment yield and energy data.[1] Recent experiments[2] and some changes in the model have improved the over-all correlation and have removed some of the discrepancies shown in Ref. 1. The calculations in Sec. II may best be described as a method of correlating the available mass, energy, and yield data in order to predict other quantities, such as independent yields. In Sec. III we introduce a set of assumptions about the fission mechanism itself, in order to deduce further properties of the U^{236} fragments. Some of the results of the Sec. II calculation are used as input to the model in Sec. III.

II. EMPIRICAL CORRELATION OF ENERGY AND YIELD DATA

Modifications in the Model

The following modifications were made in the model described in Ref. 1.

The new initial mass yield data of Schmitt *et al.*[2] were used as input. The variances of the kinetic-energy distribution as a function of mass were also taken from the work of Schmitt *et al.*

The formula for partitioning the excitation-energy variance between the two fragments was changed somewhat. It was assumed that the variance of each fragment is proportional to $(\bar{\nu}+0.4)$, instead of $\bar{\nu}$, where $\bar{\nu}$ is the average number of neutrons emitted from the fragment. This change was made because $(\bar{\nu}+0.4)$ is more nearly proportional to the fragment excitation energy (see Appendix B of Ref. 1).

The method for determining the number of neutrons emitted from a fragment is basically the same as in Ref. 1. That is, a fragment is assumed to emit a neutron whenever enough energy is available. However, some changes were made in the details of the calculation. Even-even nuclei were assumed to have 2.2 MeV more excitation energy than odd-odd nuclei because of pairing effects. The pairing energy was chosen on the basis of Cameron's work.[3] The probability for emitting no neutrons was determined by integrating the excitation-energy distribution over the energy range below the neutron separation energy. The excitation-energy distribution was then decreased by the neutron binding energy plus 1.2 MeV, the average neutron kinetic energy, and the mass number decreased by one. Also, the variance of the excitation-energy distribution was increased by 1.27 $(\text{MeV})^2$, which is the neutron kinetic-energy variance. Again, the probability of emitting no neutrons was computed, and the process continued until the probability for emitting six neutrons from the original fragment was determined. This method is an improvement over the earlier one, because it takes into account the smearing of the excitation-energy distribution by successive neutron emission. Mathematically, Eq. (4) in Ref. 1 is replaced by $p_\nu = E_\nu - E_{\nu-1}$. The quantity E_ν is defined by

$$E_\nu = \frac{1}{(2\pi\sigma_\nu^2)^{1/2}} \int_{-\infty}^{S_n(Z,M-\nu)} dW\, e^{-[W-W_\nu(Z,M)]^2/2\sigma_\nu^2}, \qquad (1)$$

where

$$W_\nu(Z,M) = W_0 + \Delta - 1.21(\nu) - \sum_{n=0}^{n=\nu-1} S_n(Z,M-n)$$

and

$$\sigma_\nu^2 = \sigma_W(M)^2 + 1.27(\nu).$$

All energies are in MeV and Δ is the pairing-energy correction.

The input data for the charge distribution also were changed. The new curve for the most probable charge is shown in Fig. 1. This is a theoretical curve derived by Fong.[4] It was obtained by maximizing the excitation energy with respect to charge, essentially as described in Appendix A of Ref. 1, except that the Wing-Fong mass formula[5] was used to obtain the mass variation. This

[1] J. M. Ferguson and P. A. Read, Phys. Rev. **139**, B56 (1965).
[2] H. W. Schmitt, J. H. Neiler, and F. J. Walter, Phys. Rev. **141**, 1146 (1966).
[3] A. G. W. Cameron, Can. J. Phys. **36**, 1040 (1958).
[4] P. Fong (private communication.)
[5] J. Wing, Bull. Am. Phys. Soc. **9**, 412 (1964); J. Wing and J. D. Varley, Argonne National Laboratory Report No. ANL-6886, 1964 (unpublished).

method of deriving the most probable charge follows naturally from the statistical theory of fission. Some of the features of the curve are corroborated by the radiochemical work of Strom *et al.*[6] A curve for Z_0 could also be calculated using the mass data of Myers and Swiatecki.[7] We have not yet investigated this alternative.

When the new curve for Z_0 was put into the calculation, it was found that a charge distribution even narrower than that used in Ref. 1 was needed to fit the radiochemical data. Therefore, the standard deviation of the initial charge distribution, σ_Z, was changed from 0.55 to 0.45.

The neutron-emission input data also require some discussion. The data of Apalin *et al.*[8] were used. Terrell[9] has pointed out that in experiments of this sort, experimental mass resolution must be carefully accounted for, since it may dominate the results in regions of very low yield. Therefore, the results for these regions should be used with some reservation. Improved neutron data would be very useful. It is encouraging, however, that the calculated neutron numbers of Gordon and Aras[10] (using kinetic-energy data as input) are in fairly good agreement with the results of Apalin *et al.* except near symmetric fission.

Results of the Modifications

Figure 2 shows the new radiochemical mass-yield results, compared with experimental results.[11] Compared with Fig. 1 of Ref. 1, the calculated yields at symmetry and at the extreme wings of the curve are much closer to the experimental values. The improvement is due entirely to the new initial yield data used as input.

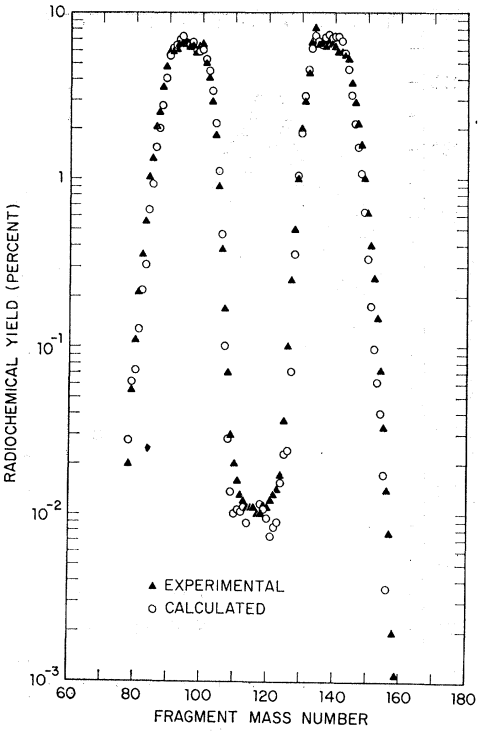

FIG. 2. Comparison of calculated and measured radiochemical mass yields. The open circles are the radiochemical mass yields calculated in this paper, and the triangles are measured and interpolated values taken from the compilations of Farrar *et al.* (Ref. 11).

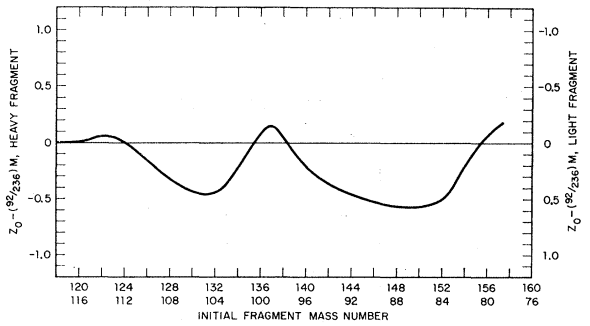

FIG. 1. Values of the most probable charge, Z_0, as calculated by Fong (Ref. 4). The quantity Z_0 is an estimate of the average number of protons for fragments of mass M before neutron emission. The values have been presented as $Z_0-(92/236)M$, in the manner of Wahl (Ref. 13) in order to emphasize the derivation from proportionate charge and mass division of the fragments.

The calculated kinetic energies are compared with experiment in Fig. 3. The masses used in obtaining the calculated curve are those of Wing and Fong.[5] The agreement is again much better than shown in Ref. 1. In this case the improvement is due to changes in the experimental results[2] rather than in the calculations. In these data the dip at symmetry is much less pronounced than in previous data. This feature is confirmed by the range experiments of Aras *et al.*[12] The discrepancy at symmetry is reduced from about 25 MeV to about 10 MeV. Elsewhere the discrepancies are of the order of a few MeV. Except at extreme asymmetry the calculated values are higher than the experimental values. This is consistent with the calculated gamma-ray energies being lower than experiment; presumably about 3 MeV of the calculated kinetic energy should appear as gamma-ray energy instead. Also, the discrepancy between the calculated and experimental curve is within the differences between various mass formulas. If Cameron's mass values[3] are used, for example, the agreement at symmetry and near the peak

[6] P. O. Strom, D. L. Love, A. E. Greendale, A. A. Delucchi, D. Sam, and N. E. Ballou, Phys. Rev. **144**, 984 (1966).
[7] W. D. Myers and W. J. Swiatecki, University of California Report No. UCRL-11980, Berkeley, California, 1965 (unpublished).
[8] V. F. Apalin, Yu N. Gritsyuk, I. E. Kutikov, V. I. Lebedov, and L. A. Kikaelyan, Nucl. Phys. **55**, 249 (1964).
[9] J. Terrell, Phys. Rev. **127**, 880 (1962).
[10] G. E. Gordon and N. K. Aras, IAEA Symposium on the Physics and Chemistry of Fission, Salzburg, Austria, 1965; Paper SM-60/48 (unpublished).
[11] H. Farrar and R. H. Tomlinson, Nucl. Phys. **34**, 367 (1962); H. Farrar, H. R. Fickel, and R. H. Tomlinson, Can. J. Phys. **40**, 1017 (1962).
[12] N. K. Aras, M. P. Menon, and G. E. Gordon, Nucl. Phys. **69**, 337 (1965).

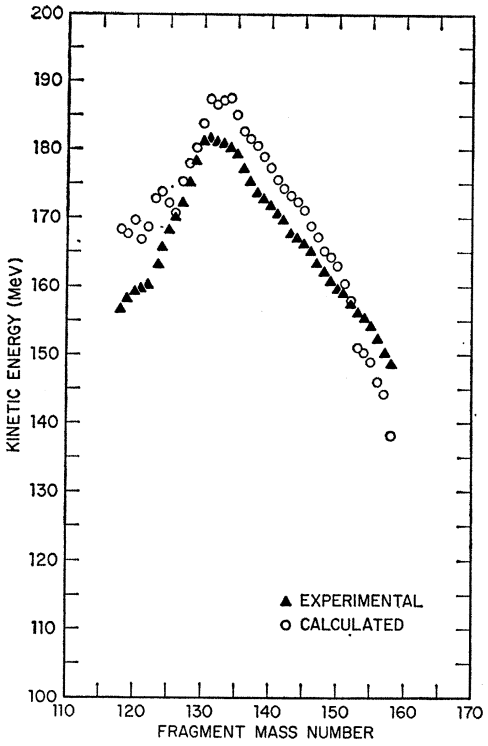

FIG. 3. Comparison of calculated and measured kinetic energies. The open circles are the calculated average kinetic energies for each fragment pair, plotted against the mass of the heavy fragment. The solid points are the experimental data of Schmitt *et al.* (Ref. 2). The calculated values were obtained by energy balance, using the semiempirical mass values of Wing and Fong (Ref. 5), and the excitation energies in Fig. 6.

is almost perfect. Therefore, the calculated curve agrees with experiment within the accuracy of the input data.

The calculated independent yields are compared with experiment in Fig. 4.[13–18] Comparing Fig. 4 with the results shown in Ref. 1, we see that the agreement is somewhat worse than before. The root-mean-square (rms) value of the log of the ratio of calculated to measured yields is 1.1 for the present calculations, compared to a factor of 1.0 obtained before. It is important to remember, however, that the work in Ref. 1 was based on an empirical Z_0 curve, while the present work used a curve derived from theory. Therefore, one would expect the former results to have a smaller average deviation. As was pointed out in Appendix A of Ref. 1, the theoretical curve is very sensitive to the semiempirical mass values. Since uncertainties of only a few tenths of a charge unit are enough to account for the observed discrepancies, we feel that the agreement between calculated and measured independent yields is good.

Both Ferguson[16] and Gordon and Aras[10] have pointed out that the width of the radiochemical charge distribution probably varies significantly with mass. Strom *et al.*[6] also give evidence for considerable structure in the charge width and Z_0 curves. This leads us to believe that better predictions could be made only with a much more complicated model. Apparently there is much interesting structure in the charge distribution which can be studied by radiochemical methods and high-resolution direct measurements.

The calculated gamma-ray energies emitted as a function of mass are shown in Fig. 5. The average gamma-ray energy per fission is calculated to be about 4 MeV, compared to 1.4 MeV per fission in Ref. 1. Thus, the new calculation comes closer to the experimental value of 7.2 MeV per fission.[19] The improvement is due to the modifications in the neutron-evaporation calculation and the use of new, smaller kinetic-energy variances as input data. The remaining discrepancies in the magnitude of the gamma-ray energy and its variation with mass is almost surely due to our assumption that excited nuclei emit neutrons whenever possible. Actually, certain features of low-energy nuclear level spectra tend to inhibit neutron emission to these levels. Gordon and Aras[10] have pointed out the importance of these effects and they obtain much better agreement

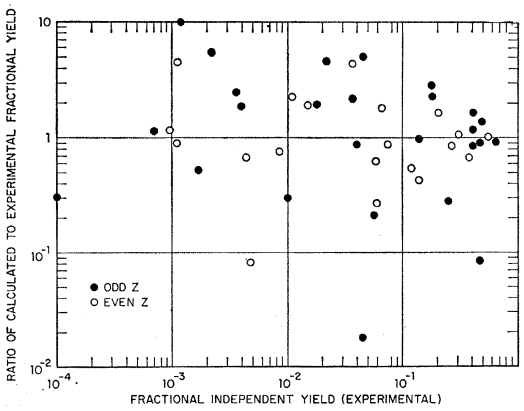

FIG. 4. Comparison of calculated and measured independent and fractional chain radiochemical yields. The fractional independent yield, given on the absicssa, is the ratio of the independent radiochemical yield to the radiochemical mass yield. In some cases the measured quantity is a fractional chain yield—the yield of all isobars with atomic number less than a given value. (In cases where the fractional chain yield is greater than one-half, the comparison was made with the fractional chain yield subtracted from unity. For such cases the latter number is more sensitive to errors and therefore is a better measure of the success of the calculation.) Each point represents a measurement taken from Refs. 6 or 12–18. The ordinate gives the ratio of our calculated fractional yield to the reported measured value.

[13] A. C. Wahl, R. L. Ferguson, D. R. Nethaway, D. E. Troutner, and K. Wolfsberg, Phys. Rev. **126**, 1112 (1962); see also references therein for earlier work.

[14] N. K. Aras and G. E. Gordon, J. Inorg. Nucl. Chem. **28**, 763 (1966).

[15] H. V. Weiss and N. E. Ballou, Phys. Rev. **139**, B304 (1965).

[16] R. Ferguson, Oak Ridge National Laboratory, Chemistry Division Annual Progress Report, 1965 (unpublished).

[17] A. C. Wahl, Progress Report No. TID-14466, Washington University, St. Louis, Missouri, 1962 (unpublished).

[18] P. O. Strom, G. R. Grant, and A. C. Pappas, Can. J. Chem. **43**, 2493 (1965).

[19] F. C. Maienschein, R. W. Peelle, R. W. Zobel, and T. A. Love, *Proceedings of the Second United Nations International Conference on the Peaceful Uses of Atomic Energy, Geneva, 1958* (United Nations, Geneva, 1958), Paper P/670.

by approximately allowing for them in their neutron evaporation calculations. Grover[20] gives a particularly good discussion of angular momentum effects on neutron-gamma competition, and it would be desirable to incorporate his ideas into our calculation. Unfortunately, the length of our computer program, with its large number of neutron-evaporation calculations, prohibits us from including such a feature at this time.

The calculated excitation energies are shown in Fig. 6. Because of the above gamma-ray effects, they probably are low by about 2 MeV.

The last results are the probabilities P_n of emitting n neutrons per fission, given in Table I. As in Ref. 1, the calculated probabilities show a significantly wider variation about the mean than do the experimental results.[21] We have no satisfactory explanation for this discrepancy. Apparently it is not due to the details of our particular model, since Gordon and Aras get the same discrepancy in their calculation.[10] See Ref. 1 for a more detailed discussion of possible contributors to this discrepancy.

III. MODEL OF THE NUCLEUS AT SCISSION

In the remainder of this paper we interpret the excitation-energy and kinetic-energy data in terms of a simple model of the nucleus at scission.

Qualitatively, the model is as follows. We assume that the nucleus at scission assumes a shape which minimizes the potential energy of the system. This potential energy contains three terms: the deformation energies of the light and heavy fragments and their mutual Coulomb energy. But, because of shell effects, one fragment is more easily deformed than the other. Closed-shell nuclei resist deformation. Consequently, the total potential energy is minimized by putting relatively more energy into the easily deformed fragment, because the higher deformation also decreases the mutual Coulomb energy, for most types of deformation. After fission, the deformation energy appears as fragment excitation energy, and the mutual Coulomb energy appears as kinetic energy. Thus, the easily deformed fragments have more excitation energy, and emit more neutrons. This would explain the shapes of the experimental kinetic-energy–versus–mass and neutron-emission–versus–mass curves.

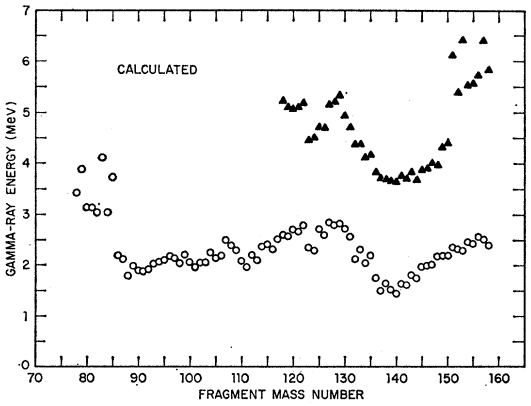

FIG. 5. Calculated gamma-ray energy emitted per fragment. The open circles give the calculated average gamma-ray energy per fragment, as a function of fragment mass. The solid triangles are the average gamma-ray energy per fragment pair, plotted against the mass of the heavier fragment.

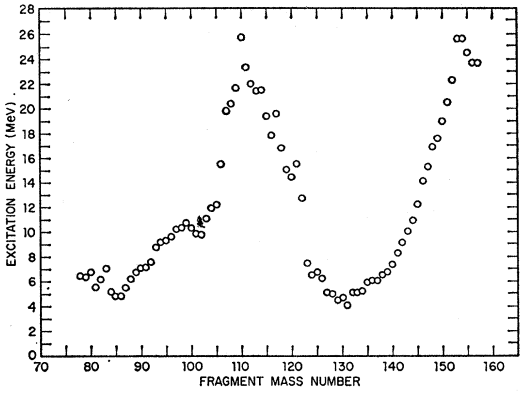

FIG. 6. Calculated fragment excitation energies. The average excitation energy per fragment pair is plotted versus fragment mass number.

These concepts of the nucleus at scission are not new. Terrell, in an earlier paper,[9] pointed out that the minima in the neutron-yield-versus-mass curve correspond to shell closures. He suggested that the stiffness of closed-shell nuclei was responsible for their small excitation energy. In later work[22] he applied a simple model in which the fragments at scission are represented as touching ellipsoids with deformation energy $E_D=\alpha(R-R_0)^2$ and mutual Coulomb energy $Z_lZ_he^2/(R_l+R_h)$. By minimizing the potential energy and using the kinetic energies and neutron emissions as input data, he derives α as a function of mass. His values of α obtained from thermal neutron fission of U^{233}, U^{235}, and Pu^{239}, and spontaneous fission of Cf^{252} agree with each other. The deformation parameter α increases dramatically near magic numbers.

TABLE I. Probabilities P_n of emission of n neutrons per fission.

	Calculated	Measured (Ref. 21)
P_0	0.077	0.027
P_1	0.183	0.158
P_2	0.266	0.339
P_3	0.246	0.305
P_4	0.158	0.133
P_5	0.059	0.038
P_6	0.015	(−0.001)

[20] J. R. Grover, Phys. Rev. **127**, 2142 (1962).

[21] B. C. Diven, H. C. Martin, R. F. Tashek, and J. Terrell, Phys. Rev. **101**, 1012 (1956).

[22] J. Terrell, *Physics and Chemistry of Fission* (International Atomic Energy Agency, Vienna, 1965), Vol. II.

Vandenbosch,[23] using a similar model, showed that by using the U^{236} kinetic energy and neutron data as input, he could reproduce the kinetic energies for Cf^{252}, Ac^{228}, and At^{213}. Also, he showed that the resulting curve for the stiffness parameter versus mass correlated well with that derived from nuclear-level structure information.

Brunner and Paul,[24] in formulating a model of the fission flarrier, came to the conclusion that asymmetric fission was due to variations in the height of the barrier. They ascribe these variations to differences in the deformation of the fragments, which in turn are due to the stiffness of closed-shell nuclei.

Fong[25] used stiffness parameters (for quadrupole deformation) extrapolated from nuclear-structure data as input to his earlier statistical theory of fission. He was able to reproduce the experimental kinetic-energy–versus–mass curve for U^{236}, and also obtained a saw-tooth shape for the excitation-energy–versus–mass curve, in agreement with the neutron data. The asymmetric yields are not predicted. However, Fong points out that the energy changes needed to predict asymmetric fission are within the errors of the approximate expression for the deformation energy.

Schmitt[26] has obtained deformability parameters using only the kinetic-energy data for U^{236} and Cf^{252}. He assumes that the fragments at scission are slightly separated spheroids with their potential energy minimized. The shape of Schmitt's curve for the deformability parameter versus mass agrees, at least qualitatively, with those curves obtained from neutron-emission data or from nuclear-structure data.

In the following we use the same general approach as in the above works: We assume that at scission the potential energy is minimized. We combine this assumption with a simplified model of the nuclear shape at scission to obtain deformation parameters and kinetic energies.

We assume that the fragments at scission can be represented by a spherical harmonic expansion about a spherical shape:

$$R_i=R_{0i}\Big(1+\sum_{\lambda=2}^{5}\alpha_{\lambda i}Y_{\lambda 0}(\cos\theta)\Big). \tag{2}$$

(The index i identifies the fragment mass, throughout this paper.) The upper limit of 5 for λ is taken from semiqualitative considerations.[27] We assume that the wavelength of the deformation must be larger than the size of a nucleon; this is true only for $\lambda\lesssim 5$. Our cutoff is therefore plausible, but not rigorously established, and should be regarded merely as a simplifying assumption. The effect of varying the cutoff of the series in λ is discussed in the Appendix.

In order to continue we must find an expression for the potential (Coulomb plus deformation) energy of the fragments. For this purpose we use a modification of an expression derived by Wilets.[27] Wilets' first-order expression for the energy change due to the deformation of the ith fragment, in contact with its complementary fragment i', is

$$D_i'=\sum_\lambda\left\{\frac{S_{0i}}{8\pi}(\lambda-1)(\lambda+2)\alpha_{\lambda i}^2-\frac{Z_1Z_2e^2}{(R_{0i}+R_{0i'})}\left[\frac{R_{0i}}{R_{0i}+R_{0i'}}\right.\right.$$
$$\left.\left.-\left(\frac{3}{2\lambda+1}\right)\left(\frac{R_{0i}}{R_{0i}+R_{0i'}}\right)^\lambda\right]\left(\frac{2\lambda+1}{4\pi}\right)^{1/2}\alpha_{\lambda i}\right\}, \tag{3}$$

where $(R_{0i}+R_{0i'})$ is the sum of the radii of the ith fragment and its complementary fragment i'. The quantity S_{0i} is the surface energy of the ith fragment when it is spherical:

$$S_{0i}=4\pi R_{0i}^2\tau_i, \tag{4}$$

where τ_i is the surface tension.

Equation (3) includes the increase in surface tension energy due to deformation, and also the change in mutual Coulomb energy due to deformation. Wilets derives this expression as an expansion to order x^2, where x is the fissionability parameter *of the fragments*, and is of the order of one-half.

The above expression refers to touching fragments. In our preliminary analysis we found that this expression consistently gives kinetic energies high by about 20%, using $r_0=1.2$ F. To obtain reasonable values for the kinetic-energy one must either take $r_0=1.5$ F, which is unreasonably high, or one must assume that the fragments "at scission" are separated by a small distance Δ. We chose the latter assumption. (Another possibility would be to assume that the fragments are polarized; this possibility was not considered in this work.) A value of $\Delta=2.4$ F was used. This separation may be rationalized on the basis of the width of the nuclear surface. The nuclear-density distribution does not have a sharp boundary but drops from a large to a small value over a distance of about 2 F. Hence, the 2.4-F separation between the "surfaces" of the fragments does not represent a complete separation between the fragments. They still touch, in that their density distributions overlap. The introduction of a spacing requires that in Eq. (3) the quantity $(R_{0i}+R_{0i'})$ be replaced by the quantity $(R_{0i}+R_{0i'}+\Delta)$.

A second modification to Eq. (3) is the inclusion of a term to account for the change in Coulomb self-energy of each fragment[28] to order α^2. The additional coefficient

[23] R. Vandenbosch, Nucl. Phys. **46**, 129 (1963).
[24] W. Brunner and H. Paul, Ann. Physik, **6**, 267 (1960); **7**, 326 (1961); **7**, 333 (1961).
[25] P. Fong, Phys. Rev. Letters **11**, 375 (1963).
[26] H. W. Schmitt, Bull. Am. Phys. Soc. **10**, 1099 (1965).
[27] L. Wilets, *Theories of Nuclear Fission* (Clarendon Press, Oxford, England, 1964).
[28] See, for example, O. Nathan and S. G. Nilsson, *Alpha-, Beta-, and Gamma-Ray Spectroscopy* (North-Holland Publishing Company, Amsterdam, 1965), Chap. X.

of $\alpha_{\lambda i}^2$ is

$$-\frac{3}{4\pi}\frac{(\lambda-1)}{(2\lambda+1)}\frac{Z_i^2e^2}{R_{0i}}.$$

This coefficient can be as much as 50% of the surface-tension coefficient of $\alpha_{\lambda i}^2$, and so needs to be included.

The modified expression for the energy due to the deformation of the ith fragment becomes

$$D_i=\sum_\lambda\left\{\left[\frac{S_{0i}}{8\pi}(\lambda-1)(\lambda+2)-\frac{3}{4\pi}\frac{(\lambda-1)}{(2\lambda+1)}\frac{Z_i^2e^2}{R_{0i}}\right]\alpha_{\lambda i}^2 - \frac{Z_iZ_{i'}e^2}{(R_{0i}+R_{0i'}+\Delta)}\left[\frac{R_{0i}}{(R_{0i}+R_{0i'}+\Delta)}-\frac{3}{(2\lambda+1)}\right]\times\left(\frac{R_{0i}}{(R_{0i}+R_{0i'}+\Delta)}\right)^\lambda\left[\left(\frac{2\lambda+1}{4\pi}\right)^{1/2}\alpha_{\lambda i}\right]\right\}. \quad (5)$$

The complete expression of the potential energy of the fragment pair i, i' at scission is

$$V=E_{\mathrm{Co}}+S_{0i}+S_{0i'}+D_i+D_{i'}. \quad (6)$$

In this expression E_{Co} is the Coulomb energy of the underformed fragments,

$$E_{\mathrm{Co}}=\frac{Z_iZ_{i'}e^2}{(R_{0i}+R_{0i'}+\Delta)}+\frac{3Z_i^2e^2}{5R_{0i}}+\frac{3Z_{i'}^2e^2}{5R_{0i'}}, \quad (7)$$

and S_{0i} is defined in Eq. (4).

The radii were taken to be $R_{0i}=1.2A_i^{1/3}$ F, and the separation Δ was taken to be 2.4 F, on the basis of the kinetic energies. We are left with the problem of determining the surface-tension parameters, $4\pi r_0^2\tau_i$. (We express surface tension at $4\pi r_0^2\tau_i$ MeV, because this quantity corresponds to the surface coefficient A_s in the usual semiempirical mass formula.) As was indicated above, it is essential that we take into account the variation of this parameter with mass number. Therefore, we left the quantities τ_i as free parameters, to be determined from the excitation energies calculated in the first section of this paper. In determining these parameters we assumed that, for a given nuclide, the surface tension is the same for all multipoles.

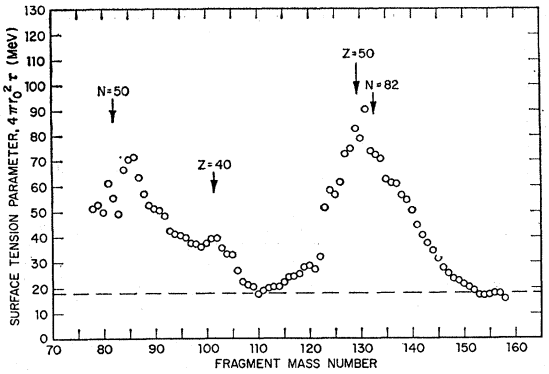

FIG. 7. Surface-tension parameters calculated in this work. The ordinate is equivalent to the coefficient A_s in the usual semiempirical mass formula; i.e., the surface energy of an undeformed fragment of mass A_i is given by $4\pi r_0^2\tau_i A_i^{2/3}$.

Also, we assume that at scission the entire excitation energy of each fragment is tied up in deformation energy. Then we may equate the energies W_i determined in Sec. II with the theoretical expression for the deformation energy:

$$W_i=\sum_\lambda\left[\frac{(4\pi r_0^2\tau_i)A_i^{2/3}}{8\pi}(\lambda-1)(\lambda+2) - \frac{3}{4\pi}\frac{(\lambda-1)}{(2\lambda+1)}\frac{Z_i^2e^2}{R_{0i}}\right]\alpha_{\lambda i}^2. \quad (8)$$

With all these assumptions, the evaluation of the potential-energy parameters is straightforward. The potential energy [Eq. (6)] is minimized with respect to each mode of deformation of each fragment,

$$\partial V/\partial\alpha_{\lambda i}=0, \quad (9)$$

for each λ and i. Equations (5) through (9) may be solved for τ_i. (The solution is a fourth-order polynomial in τ_i. It is easily shown, however, that all but the largest of the four roots correspond to surface tensions which would make the fragment itself unstable to fission. Therefore, the quantities τ_i were found by an iterative method which coverges on the largest root.) With this parameter determined we can solve for the spherical harmonic coefficients and the kinetic (mutual Coulomb) energies:

$$\alpha_{\lambda i}=\left(\frac{Z_iZ_{i'}e^2}{r_0}\right)\left(\frac{4\pi}{2\lambda+1}\right)^{1/2}\left(\frac{R_{0i}}{R_{0i}+R_{0i'}+\Delta}\right)^2\left[1-\frac{3}{(2\lambda+1)}\left(\frac{R_{0i}}{R_{0i}+R_{0i'}+\Delta}\right)^{\lambda-1}\right]\Bigg/ \left[(4\pi r_0^2\tau_i)A_i\frac{(\lambda-1)(\lambda+2)}{(2\lambda+1)}-\frac{6(\lambda-1)}{(2\lambda+1)^2}\left(\frac{Z_i^2e^2}{r_0}\right)\right] \quad (10)$$

and

$$T=\frac{Z_iZ_{i'}e^2}{(R_{0i}+R_{0i'}+\Delta)}\left\{1-\sum_{i=i,i'}\frac{R_{0i}}{(R_{0i}+R_{0i'}+\Delta)}\sum_\lambda\left[1-\frac{3}{(2\lambda+1)}\left(\frac{R_{0i}}{R_{0i}+R_{0i'}+\Delta}\right)^{\lambda-1}\right]\left(\frac{2\lambda+1}{4\pi}\right)^{1/2}\alpha_{\lambda i}\right\}. \quad (11)$$

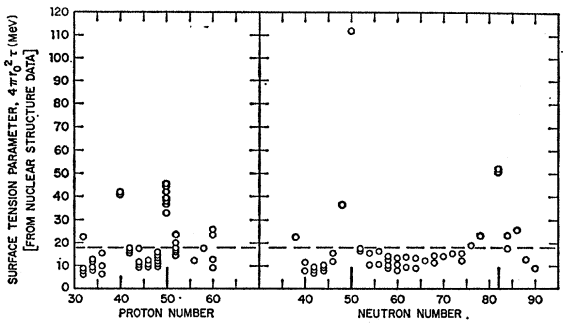

FIG. 8. Surface-tension parameters calculated from nuclear structure data. The ordinate is equivalent to that in Fig. 7, but is calculated from the properties of the first excited states of even-even nuclei, assuming a simple vibrational model for the mode of excitation. The data are plotted versus proton and neutron numbers to emphasize shell effects. (Closed shells are denoted by heavy marks on the abscissa.) Nuclides with closed neutron shells are omitted from the plot versus proton number, and vice versa, to help isolate proton and neutron shell effects.

Thus, the surface-tension parameters, deformations, and kinetic energies of each fragment pair can be determined from the fragment excitation energies (Fig. 6).

The surface-tension parameters obtained from these calculations are shown in Fig. 7. The surface-tension parameter shows the strong dependence with mass number found by others.[22–26] It is generally higher than the semiempirical mass value, as Terrell also found.

In Fig. 8 we have plotted a set of surface-tension parameters deduced from nuclear-structure data.[29–31] These data clearly show a strong effect at closed shells, as is implied by the curve obtained from our fission model. The absolute values of the nuclear-structure parameters are generally lower by a factor of 2 to 4 than those we have found. This difference is not too unreasonable. Any further refinement in our model, such as including higher terms in the series or assigning some of the excitation energy to internal energy, would reduce our values. Furthermore, the nuclear-structure values themselves are open to question. They are calculated on the assumption that the first excited state of the even-even nuclides in this region is formed by the nuclear surface making quadrupole vibrations about a spherical shape.[28] This model is not completely correct for any nucleus, and is certainly very poor, for some, if not most, of the nuclides represented in Fig. 8. For example, the energy spectra above the first excited state does not resemble that of simple vibrators in most of the nuclides considered. Also, note that the nuclear-structure values correspond to deformation energies of 1 MeV or less, while the fission values are for deformation energies of the order of 10 MeV. It is unlikely that a single value of the surface-tension parameter fits over this range of deformations.

The kinetic energies obtained from Eq. (11) are compared with experiment in Fig. 9. The agreement is generally good, with the average discrepancy being about 5 MeV, and the shapes of the curves being very similar. The disagreement is highest for symmetric and very asymmetric fission. Recall that the calculation is based on empirically determined excitation energies, and these energies are most uncertain at symmetric and very asymmetric fission. The discrepancies for the extremes of the kinetic-energy curve correspond to changes in the excitation energies of about 5 MeV, which is not beyond the limits of accuracy of W_i, although it is rather high.

In addition, we have calculated the spherical harmonic coefficients $\alpha_{\lambda i}$. Instead of tabulating these values, we have plotted the shapes of the fragments, for three mass ratios, in Fig. 10. In each case we have included a curve of the *saddle-point* shape for U^{236} fission as calculated by Lawrence,[32] and by Cohen and Swiatecki.[33] (The two results are numerically almost identical.)

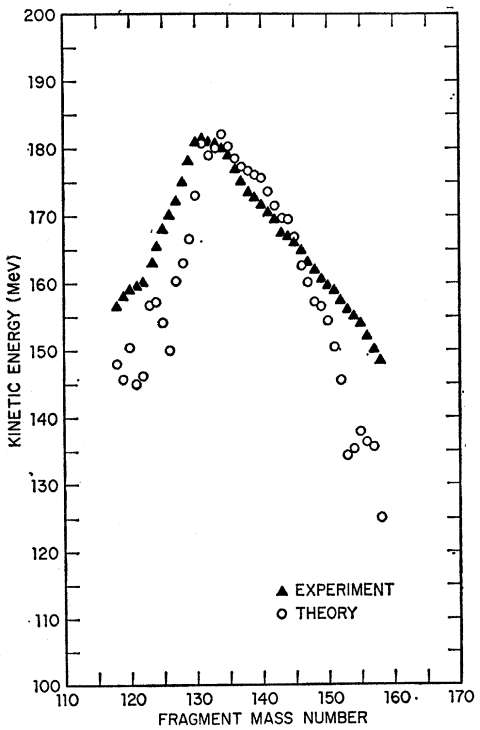

FIG. 9. Comparison of experimental kinetic energies with those calculated from Eq. (11) of this paper. The open circles are the calculated values and the solid triangles are the values measured by Schmitt *et al.* (Ref. 2). These calculations are not to be confused with those of Fig. 3, which are based only on energy balance.

[29] K. Alder, A. Bohr, T. Huus, B. Mottelson, and A. Winther, Rev. Mod. Phys. **28**, 432 (1956).

[30] P. H. Stelson and F. K. McGowan, Phys. Rev. **110**, 489 (1958).

[31] *Nuclear Data Sheets*, compiled by K. Way *et al.* (Printing and Publishing Office, National Academy of Sciences—National Research Council, Washington 25, D. C., 1964), NRC 6-4-101.

[32] J. P. Lawrence, Phys. Rev. **139**, B1227 (1965).

[33] S. Cohen and W. J. Swiatecki, Ann. Phys. (N.Y.) **22**, 406 (1963).

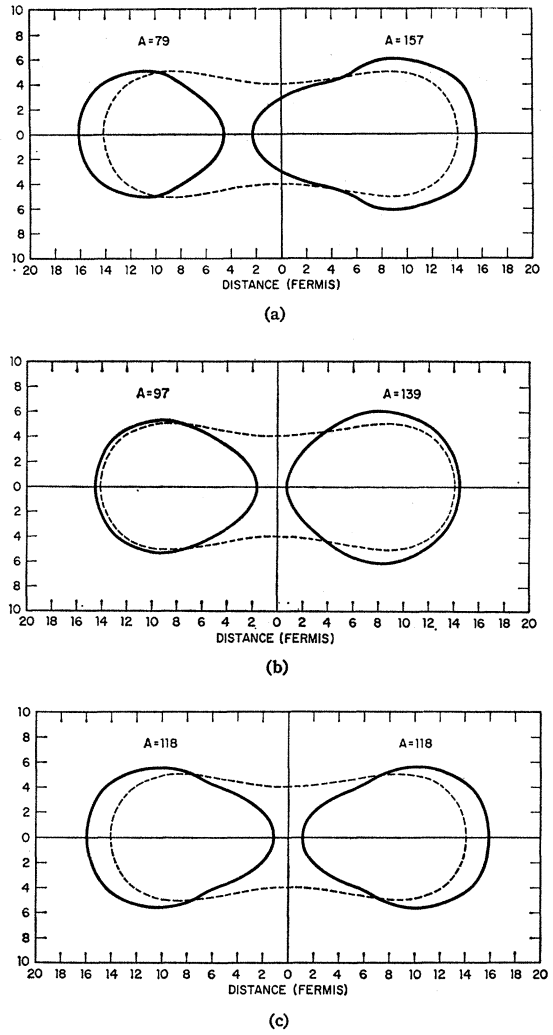

FIG. 10. Shapes of the fragments *at scission*, as calculated from Eqs. (2) and (10). The nuclear surfaces are of course not sharp boundaries, as shown, but are diffuse over a distance of about 2 F. The calculated shapes are shown for three mass ratios, corresponding to very asymmetric, asymmetric (very probable), and symmetric fission. For comparison, the calculated *saddle point* shape calculated by Lawrence (Ref. 32) and by Cohen and Swiatecki (Ref. 33) is shown as a dashed line.

If one is to interpret the shapes further (and this really goes beyond the scope of our simple calculation), the implication is that there is little further elongation between saddle point and scission. The main change is a necking in of the fissioning nucleus. This picture appears to have features similar to that presented by Cohen and Swiatecki,[33] and by Milton[34]: For nuclei with $x \gtrsim 0.67$ the saddle point is already quite close to the scission shape. Our model also implies somewhat greater elongation at scission for symmetric and very asymmetric fission than for intermediate-mass ratios.

[34] J. C. D. Milton, *Advanced Course on Nuclear Physics with Thermal Neutrons* (Institut for Atomenergi, Kjeller, Norway, 1963).

IV. CONCLUSIONS

In the first part of the paper we demonstrated that the available mass, energy, and yield data can be correlated successfully with a simple semiempirical calculation. It appears that an improved correlation requires improved neutron-emission data and more accurate semiempirical mass predictions. All the evidence we have indicates that the charge-mass distribution is not a simple, smoothly varying function, but has a great deal of structure. More extensive radiochemical data, or higher resolution initial yield measurements should reveal some very interesting features due to odd-even effects and closed-shell effects.

The major portion of this work involved applying a simple model of the nucleus at scission to U^{236}. The fragment excitation energies were used as input, and from these were calculated the surface-tension parameters, the kinetic energies, and the shapes of the fragments as a function of mass. The following are the major assumptions made in the calculation: (i) the potential energy is minimized at scission; (ii) the entire fragment excitation energy is tied up in deformation energy at scission; (iii) the surface-tension parameter, $4\pi r_0^2\tau_i$, is the same for all modes (multipoles) of deformation; (iv) the shape of each fragment can be represented by a spherical harmonic expansion cut off at $\lambda=5$; (v) Eq. (5) adequately approximates the deformation energy as a function of the spherical-harmonic coefficients; (vi) the fission fragments are separated by a distance $\Delta=2.4$ F (separation between mean radii) at scission.

Obviously many or all of these assumptions are open to question, so that the model is really only an interesting hypothesis. For example, the potential energy need not be minimized at scission; the shape of the potential barrier leading to scission might favor development of a shape not minimizing the potential energy at scission. Also, some of the excitation energy is no doubt tied up in internal excitation, whereas we have assumed that the nucleus is "cold" at scission, so that this internal energy is small.

The validity of assumptions (iv) and (v) depends, in part, on how big the coefficients α_λ are, and how rapidly they diminish as λ increases from 2 to 5. These considerations are important because the terms neglected in Eq. (5) involve higher order terms in α_λ and other terms for higher values of λ. A discussion of the choice of cutoff in λ is given in the Appendix. For the most deformed nuclei α_2 is about 0.5. More typically it is 0.1. The value of α_5 is generally a factor of 4 to 6 smaller than α_2. Although we have not examined the convergence of Eq. (5) in any detail, our feeling is that it is not a bad approximation from most cases ($\alpha_2 \sim 0.1$ or 0.2). However, it may be poor for those mass numbers which give large values α_λ. It would be worthwhile to investigate the deformation energy expansion in detail, but this is beyond the scope of the present work.

In spite of these qualifications, we feel that the

scission shapes given by Eqs. (8)–(10) are probably not far from the real shapes. (Tabulations of the entire output are available on request; we have omitted them from this paper to save space.) The excitation energies, kinetic energies, and surface-tension parameters all depend on these shapes, and it would be very difficult to obtain reasonable values for all three, as we have here, with radically different shapes.

This investigation will be extended to other nuclides, with further investigations of the validity of the model.

APPENDIX

As we pointed out in Sec. III, the cutoff of the series of Eq. (2) at $\lambda=5$ is rather arbitrary. In effect, this cutoff limits the range of shapes which we consider. Also, it affects the calculated surface-tension parameter. In fact, if the series went to infinity, the surface-tension parameter calculated from Eqs. (5) through (9) would become infinite, and the fragments would approach spherical shapes with a separation Δ. Since it is obvious that the cutoff affects the results, we discuss here the question of how sensitive the results are to the particular choice of the cutoff.

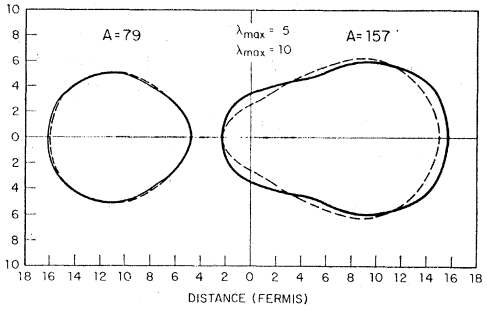

FIG. 11. Comparison of shapes calculated for different cutoff values for the series of Eq. (2). The solid curve is for maximum $\lambda=10$, while the dashed line represents maximum $\lambda=5$, the value used in the main body of the paper.

To investigate this question we extended the calculations on the fragment pair $A_1=79$, $A_2=157$. Since $A=157$ is the most deformed fragment, it represents an extreme case. The results of the calculation for maximum $\lambda=10$ are shown in Fig. 11. The shapes are not radically changed. The values of $R(\theta)$ for cutoffs at $\lambda=5$ and $\lambda=10$ differ typically by 10% or less for $A=157$. In general, the shapes are not extremely sensitive to the choice of cutoff, varying slowly for cutoffs from $\lambda=4$ to $\lambda=10$ or higher.

The surface-tension parameters increase by about 30% as the cutoff is increased from $\lambda=5$ to $\lambda=10$. They change rather uniformly, so that the effect of using $\lambda=10$ as the cutoff would increase the scale of Fig. 7, without significantly changing the shape of the curve. Increasing the cutoff by one term changes the values by only a few percent.

To summarize, the results of the model depend on the number of Legendre polynomials used to represent the shape. In effect, this cutoff is part of the model. However, the results vary slowly with the choice of cutoff, and they would be at least qualitatively the same if the number of terms was more than doubled.

If the series were extended to infinity, however, the shape would become spherical and the surface tension would approach infinity in such a manner as to keep the deformation energy finite.